Lanosterol Synthase Prevents EMT During Lens Epithelial Fibrosis Via Regulating SREBP1

Pengjuan Ma, Jingqi Huang, Baoxin Chen, Mi Huang, Lang Xiong, Jieping Chen, Shan Huang, and Yizhi Liu

State Key Laboratory of Ophthalmology, Zhongshan Ophthalmic Center, Sun Yat-Sen University, Guangzhou, China

Correspondence: Shan Huang, Zhongshan Ophthalmic Centre, Sun Yat-Sen University; No.7 Jinsui Road, Guangzhou 510060, China; huangsh29@mail.sysu.edu.cn.

PM and JH contributed equally.

Received: June 21, 2023
Accepted: October 25, 2023
Published: December 11, 2023

Citation: Ma P, Huang J, Chen B, et al. Lanosterol synthase prevents EMT during lens epithelial fibrosis via regulating SREBP1. *Invest Ophthalmol Vis Sci.* 2023;64(15):12. https://doi.org/10.1167/iovs.64.15.12

Purpose. Epithelial–mesenchymal transition (EMT) of lens epithelial cells (LECs) is a predominant pathological process underlying fibrotic cataracts. Here we investigated the role and mechanism of lanosterol synthase (LSS), a key rate-limiting enzyme in sterol biosynthesis, in EMT of LECs.

Methods. Human lens epithelial explants, primary rabbit LECs, and whole rat lenses were treated with TGFβ2. RNA-sequencing was conducted to explore genetic changes during fibrosis of human lens epithelial explants. Loss- and gain-of-function studies were performed in primary LECs to investigate roles and mechanisms of LSS, lanosterol and sterol regulatory element binding transcription protein 1 (SREBP1) in EMT. Rat lenses were applied to evaluate the potential effect of lanosterol on lens fibrosis. Expression of LSS, SREBP1, EMT-related regulators, and markers were analyzed by Western blot, qRT-PCR, or immunofluorescent staining.

Results. LSS and steroid biosynthesis were downregulated in TGFβ2-induced lens fibrosis. LSS inhibition directly triggered EMT by inducing Smad2/3 phosphorylation and nucleus translocation, an overexpression of LSS protected LECs from EMT by inhibiting Smad2/3 activation. Moreover, LSS inhibition decreased the expression of SREBP1, which regulated EMT via intervening TGFβ2/Smad2/3 transduction. Furthermore, lanosterol protected LECs from EMT caused by both TGFβ2 treatment and LSS inhibition via suppressing Smad2/3 activation and maintained lens transparency by preventing fibrotic plaques formation.

Conclusions. We first identified that LSS protected LECs from EMT and played an antifibrotic role to maintain lens transparency. Additionally, lanosterol and sterol biosynthesis regulation might be promising strategies for preventing and treating fibrotic cataracts.

Keywords: lens epithelial cells, epithelial–mesenchymal transition, lanosterol synthase, lanosterol

The crystalline lens is a transparent and biconvex organ with light transmitting and refraction properties, composed of lens epithelial cells (LECs) and lens fiber cells (LFCs). Opacification of the lens, also known as cataract, is the leading cause of vision loss worldwide.[1] As the major cells with transcriptional and metabolic activities in adult lens, the LECs are essential for lens formation and lifelong transparency maintenance.[2]

Various factors, such as radiation, metabolic disorders, ocular trauma, inflammation and intraocular surgery can disturb the homeostasis of LECs and result in lens opacity.[1] The epithelial–mesenchymal transition (EMT) of LECs is a predominant pathological biological process in fibrotic cataracts, including anterior subcapsular cataract and posterior capsule opacification.[3] During lens fibrosis, the injured LECs transdifferentiate into mesenchymal cells with increased proliferation and invasive migration to form fibrotic plaques underneath the lens capsule and lead to capsule wrinkling.[4] Further, loss of epithelial function may destroy the homeostasis and transparency of the lens cortex and nucleus, leading to different degrees and types of cataracts.

The abnormally activated TGFβ signals have been shown to induce EMT in fibrotic diseases and TGFβ2 is detected as the major isoform in the lens microenvironment to trigger lens fibrosis.[5] Upon injury, such as with ocular surgery and trauma, TGFβ2 in the aqueous humor turns from a latent state to an active state and increases significantly to activate the downstream signals such as the canonical TGFβ2/Smad2/3 pathway to induce the expression of EMT-related genes, leading to the mesenchymal transition of LECs.[6–10] Thereafter, the LECs lose their epithelial morphology, apical-basal polarity and epithelial cell-to-cell junctions formed by zonula occludens 1 (ZO1) and E-cadherin (E-cad), and obtained mesenchymal phenotypes with an elongated and spindle-like shape, accompanied by increasing expression of mesenchymal cytoskeletal proteins, such as α-smooth muscle actin (α-SMA), and excessive secretion of extracellular matrix, including fibronectin (FN), driving the formation of the fibrotic plaques and resulting in lens opacity.[11]

The steroid biosynthesis and metabolic pathways have been confirmed to be involved in EMT during various tissue fibrosis and tumor metastasis.[12–15] As an essential component of cellular membranes, cholesterol has been reported to be critical for lens development and long-term lens transparency maintenence.[16,17] Lanosterol synthase (2,3-oxidosqualene-lanosterol cyclase [LSS]) is a key early rate-limiting enzyme in cholesterol biosynthesis, which can catalyze the conversion of (S)-2,3-oxidosqualene to lanosterol, a critical precursor of sterols in mammals. Our previous studies have reported that mutations in *LSS* gene impair catalytic function of LSS, leading to lanosterol and cholesterol synthesis disorder, and identified that families with *LSS* mutations presented severe congenital cataracts.[18,19] Furthermore, LECs with *Lss* mutations could not exit the cell cycle to differentiate into lens fibers, resulting in failure of lens development.[19] Besides, lanosterol, the catalytic product of LSS, has been reported to restore lens transparency by redissolving the aggregates of mutated crystallins.[18] However, the role of LSS in EMT of LECs during the pathogenesis of lens epithelial fibrosis remains unclear.

Here, we first demonstrated that the LSS and sterols biosynthesis processes were decreased during TGFβ2-induced lens fibrosis. Then, we observed that knockdown of LSS could induce EMT by direct activation of Smad2/3 signaling, while overexpression of LSS alleviated TGFβ2-induced EMT by inhibiting Smad2/3 signals. Moreover, sterol regulatory element binding transcription protein 1 (SREBP1) was decreased by TGFβ2 treatment or LSS inhibition and was found to regulate EMT of LECs by attenuating the TGFβ2/Smad2/3 signaling transduction. Furthermore, we demonstrated that lanosterol treatment inhibited EMT of LECs caused by both TGFβ2 and LSS inhibition. Moreover, semi-in vivo whole lens culture studies presented that lanosterol alleviated rat lens fibrosis by maintaining lens epithelial phenotypes and lens clarity via suppressing Smad2/3 signals. Together, this study reveals LSS-related sterol biosynthesis pathway as a novel mechanism for the pathogenesis of lens epithelial fibrosis, the modulation of which might provide therapeutic strategies for the prevention and treatment of fibrotic cataracts.

Materials and Methods

RNA Sequencing Data Analysis

Our RNA sequencing data of human lens epithelial explants (HLEEs) upon TGFβ2 treatment was acquired as previously described[20] and downloaded from the Genome Sequence Archive in BIG Data Center (https://bigd.big.ac.cn/gsa/), with Project Accession No. PRJCA010973 and GSA Accession No. HRA002775. DESeq2 was used for differential gene expression analysis between two samples with biological replicates. Genes with a P value of less than 0.05 and a $|\log2\_FC|$ of 1 or greater were identified as differentially expressed genes (DEGs). The detected DEGs were further used to perform pathway enrichment analysis using Metascape.[21]

Isolation, Culture, and Treatment of Primary LECs

All animal experiments were approved by the Animal Ethics of Sun Yat-sen University, following the National Institutes of Health guide for the care and use of Laboratory animals. Primary LECs were isolated from 2-month-old New Zealand White rabbits and LECs between the third and fifth passages were used for subsequent cell experiments. All LECs were maintained at 37°C in a humidified 5% CO_2 incubator and cultured in MEM (11095080; Thermo Fisher Scientific, Waltham, MA, USA) with 10% fetal bovine serum (10099141C; Gibco, Gran Island, NY, USA), 1% nonessential amino acids (11140050; Thermo Fisher Scientific), and 1% penicillin/streptomycin (15140122; Thermo Fisher Scientific). In TGFβ2-induced EMT experiments, LECs were treated with TGFβ2 (302-B2-010; R&D Systems, Minneapolis, MN, USA) at different concentrations (2.5 ng/mL, 5 ng/mL, 10 ng/mL) for 3 days. Lanosterol (20 µM, L5768; Sigma, St Louis, MO, USA) were added to the culture medium with or without 5 ng/mL TGFβ2 for 3 days.

Transfection With siRNA and Plasmid

Primary LECs were transfected with small interfering RNAs (siRNAs) of the negative control (siNC), LSS (siLSS), and SREBP1 (siSREBP1), which were purchased from Ribobio. The pcDNA3.1-LSS (oeLS), pcDNA3.1-SREBP1 (oeSRE1) and control plasmids (oeNC) (Vigene Bioscience) were all commercially obtained. Lipofectamine 3000 agent (l3000015; Thermo Fisher Scientific) was used for siRNA and plasmid transfection, according to the manufacturer's protocol. When LECs were grown to 70% confluence, the transfection mixtures were premixed well for 15 minutes and then added into the culture medium. After transfection for 18 hours, the transfected cells were used in subsequent experiments.

Semi-In Vivo Whole Lens Culture and Treatment

Whole lenses were isolated from 3-week-old Sprague-Dawley rats as previously described.[22] The rat lenses were cultured in Dulbecco's Modified Eagle Medium (C11965500BT; Thermo Fisher Scientific) supplemented with 0.1% BSA and 1% penicillin/streptomycin. TGFβ2 (5 ng/mL)[23] and lanosterol (20 µM) were added to the culture medium, which was changed every other day. Whole rat lenses were cultured for up to 6 days and the lenses were photographed by a stereoscope.

Western Blot Analysis

Primary LECs and the anterior capsule with attached LECs from rat lenses were lysed in radioimmunoprecipitation assay buffer (P0013C; Beyotime, Shanghai, China) with phenylmethylsulfonyl fluoride and PhosStop Phosphatase Inhibitor Cocktail (04906837001; Roche, Basel, Switzerland). Bicinchoninic acid assay (P0012; Beyotime) was used to quantify protein concentrations. Equal proteins were mixed with 2× sodium dodecylsulphate sample buffer and were separated with sodium dodecylsulphate-polyacrylamide gel electrophoresis gels and transferred onto polyvinylidene difluoride membranes (IPVH00010; Merck Millipore, Burlington, MA, USA). The membranes were then blocked in 5% bovine serum albumin for 1 hour at room temperature, followed by incubation with primary antibodies (1:1000) overnight at 4°C and then with horse radish peroxidase-conjugated secondary antibodies (1:2000) for 2 hours at room temperature. Finally, the protein bands were detected and analyzed with chemiluminescence detection systems (WBKLS0500; Merck Millipore). The primary antibodies used in Western blot analysis were as follows: LSS (13715-1-AP; Proteintech, Rosemont, IL, USA),

ZO1 (61-7300; Thermo Fisher Scientific), E-cad (ab1416; Abcam, Cambridge, UK), FN (ab137720; Abcam), α-SMA (ab7817; Abcam), β-actin (3700S; Cell Signaling Technology, Danvers, MA, USA), phospho-Smad2 (3108; Cell Signaling Technology), phospho-Smad3 (9520; Cell Signaling Technology), Smad2/3 (8685; Cell Signaling Technology), and SREBP1(ab28481; Abcam).

RNA Isolation and Quantitative Real-Time PCR

Total RNA from primary LECs was collected and purified using the Rneasy Mini Kit (74104; Qiagen, Hilden, Germany), according to the manufacturer's protocol. Total RNA (1 µg) was converted to cDNA using PrimeScript RT Master Mix (RR036A; Takara Bio Inc, Kutsatsu, Japan). ChamQ SYBR Color qPCR Master Mix (Q431-02; Vazyme) was used for quantitative real-time PCR reactions on a Step One Plus real-time PCR system (Applied Biosystems, Waltham, MA, USA). The relative expression levels of mRNAs were evaluated by the $2^{-\Delta\Delta Ct}$ method and the expression levels were normalized to that of GAPDH.

Hematoxylin and Eosin Staining

The whole rat lenses were fixed with 4% paraformaldehyde for 1 hour at room temperature and embedded in optimal cutting temperature compound, which were then preserved in refrigerator. Freshly cut sections were first stained with hematoxylin solution (BA-4097; BASO Diagnostics, New Taipei City, Taiwan) to show the nuclei, rinsed in running tap water, and then counterstained with Eosin solution (BA-4098; BASO Diagnostics) to delineate the cellular cytoplasm. Finally, the images were captured by a Leica microscope (DM3000).

Immunofluorescent Staining

Primary LECs and the anterior capsule whole-mounts from rat lenses were collected after treatment. Frozen sections of rat lenses were collected as described above. These samples were fixed with 4% paraformaldehyde for 30 minutes and blocked in PBS containing 3% BSA and 0.3% Triton X-100 for 30 minutes at room temperature. Then they were incubated with primary antibodies (1:300) overnight at 4°C and fluorochrome-conjugated secondary antibodies (1:1000; Cell Signaling Technology) for 2 hours at room temperature, followed by counterstaining with DAPI. The images were captured using a Leica microscope (DM3000). The primary antibodies used in immunofluorescent staining were as follows: ZO1 (61-7300; Thermo Fisher Scientific), FN (ab2413; Abcam), α-SMA (ab7817; Abcam), p-Smad2/3 (AF3367; Affinity Biosciences, Cincinnati, OH, USA), and Smad2/3 (8685; Cell Signaling Technology).

Statistical Analyses

All the experiments were performed at least three times independently and data were presented as the mean ± SD. GraphPad Prism software was used for statistical analyses and one-way ANOVA was performed for statistical differences among more than two groups. A P value of less than 0.05 ($^{*}P < 0.05$, $^{**}P < 0.01$, and $^{***}P < 0.001$) was considered statistically significant.

Results

LSS Was Significantly Downregulated During TGFβ2-Induced Lens Epithelial Fibrosis and EMT of LECs

Based on bulk RNA sequencing technology, we explored the alternations of LSS expression in HLEEs upon exposure to TGFβ2 treatment. The comparative analysis of DEGs between the control group and human lens fibrosis group revealed that *LSS* and *SREBP1* expression decreased significantly with exposure to TGFβ2, whereas EMT-related genes, such as *FN*, *α-SMA*, and *TGFβ2*, increased significantly at transcriptional levels (Fig. 1A). To further investigate the biological processes involved in lens fibrosis, we used the detected DEGs to perform pathway enrichment analysis with the Metascape webtool. Genes decreased by TGFβ2 were predominantly enriched in sterols and lipid biosynthesis and metabolism processes accompanied by loss of cell-cell adhesion or adhesion molecules, whereas the upregulated DEGs were involved in EMT-related pathways, including the TGFβ receptor signaling and the Smads activation) (Fig. 1B).

To validate the changes of LSS expression during lens epithelium fibrosis in the RNA sequencing data, we used different concentrations of TGFβ2 (2.5 ng/mL, 5 ng/mL, and 10 ng/mL) to trigger EMT in primary LECs (Fig. 1C). Upon TGFβ2 treatment, LECs lost their epithelial phenotype with decreased ZO1 and E-cad expression, and transdifferentiated into mesenchymal cells with increased FN and α-SMA expression (Figs. 1C–F). Consistent with the RNA sequencing data, Western blot and immunofluorescent staining analysis presented a significant downregulation of LSS in TGFβ2-induced EMT of LECs (Figs. 1C, D, F). Taken together, we found that LSS was decreased during the process of lens epithelium fibrosis and EMT of LECs.

Knockdown of LSS Triggered EMT and Exacerbated TGFβ2-Induced EMT of LECs

To confirm the role of LSS in EMT of LECs and lens fibrosis, loss-of-function studies by siRNA transfection in primary LECs were used to block LSS expression. LSS protein expression was efficiently suppressed in the siLSS group compared to the siNC group (Figs. 2A, B). Notably, we observed that inhibition of LSS decreased the protein levels of epithelial markers, ZO1 and E-cad, while increased the expression of mesenchymal markers, FN and α-SMA (Figs. 2A, B). Immunofluorescent staining showed that LECs after LSS inhibition lost cell–cell junctions (such as ZO1) with increased secretion of extracellular matrix (FN) and expression of mesenchymal cytoskeletal proteins (α-SMA) (Fig. 2D). In addition, we further explored the effect of LSS inhibition on LECs with TGFβ2 treatment and found that the silencing of LSS in LECs exposed to TGFβ2 (siLSS+T2) showed a more significant loss of ZO1 and E-cad, with enhanced accumulation of FN and α-SMA compare with the siNC transfected group with TGFβ2 treatment (siNC+T2) (Figs. 2A–C). Overall, knockdown of LSS in LECs could induce EMT in LECs directly and exacerbated TGFβ2-induced EMT, indicating the essential role of LSS in maintaining epithelial phenotype of LECs.

Investigative Ophthalmology & Visual Science

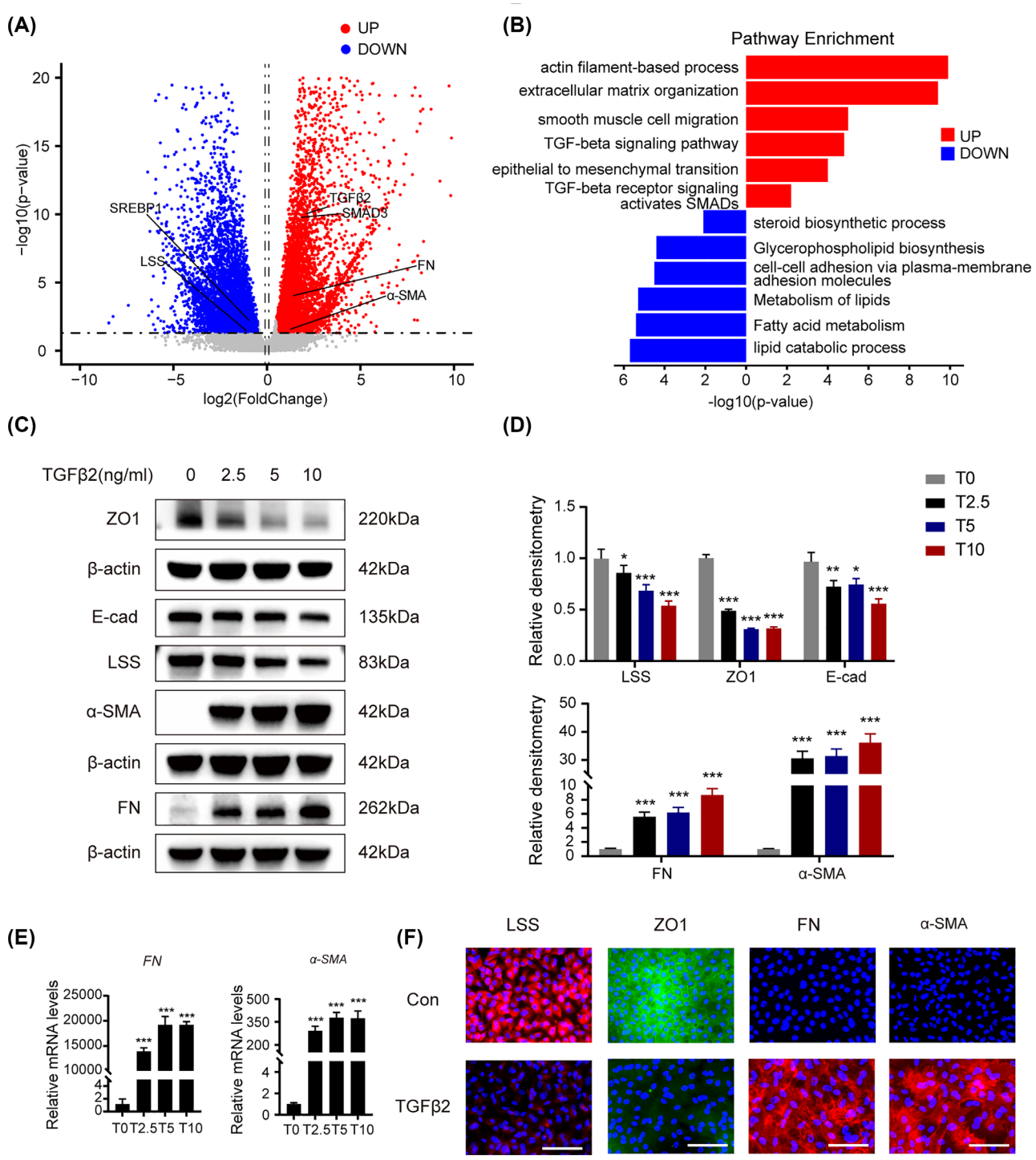

Figure 1. LSS was significantly downregulated in EMT of LECs. (**A**)Volcano plot showing upregulated and downregulated DEGs of HLEEs treated with TGFβ2 (*red* indicates upregulated DEGs, *blue* indicates downregulated DEGs). (**B**) Pathway enrichment analysis of the upregulated and downregulated DEGs (*red* indicates upregulation, *blue* indicates downregulation). (**C**, **D**) Primary LECs were treated with TGFβ2 (2.5 ng/mL, 5 ng/mL, or 10 ng/mL) for 3 days. Western blot analysis and densitometry quantification showed protein levels of LSS, ZO1, E-cad, FN, and α-SMA in LECs. (**E**) qPCR analysis of the mRNA expression levels of FN and α-SMA upon exposure to TGFβ2 with different concentrations (2.5 ng/mL, 5 ng/mL, or 10 ng/mL). qPCR analysis is presented relative to the GAPDH expression data. (**F**) Immunofluorescent staining of LSS (*red*), ZO1 (*green*), FN (*red*), and α-SMA (*red*) merged with DAPI (*blue*) in LECs of the control (Con) and TGFβ2 treatment (TGFβ2) groups. Representative images of three replicated experiments were presented: T0, 0 ng/mL TGFβ2; T2.5, 2.5 ng/mL TGFβ2; T5, 5 ng/mL TGFβ2; and T10, 10 ng/mL TGFβ2. All scale bars, 100 µm. *$P < 0.05$; **$P < 0.01$; ***$P < 0.001$. Data are shown as mean ± SD ($n = 3$).

Investigative Ophthalmology & Visual Science

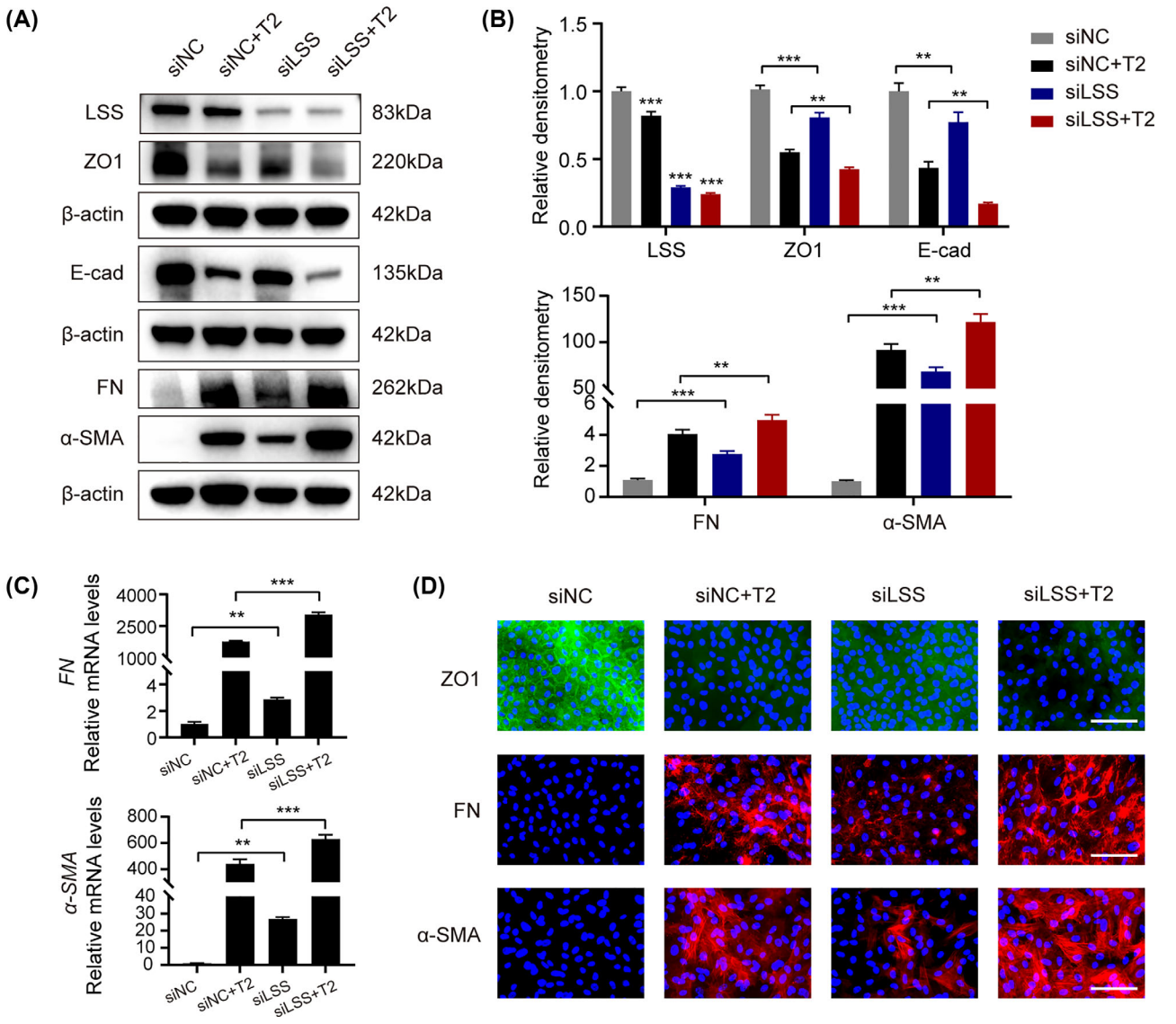

Figure 2. LSS inhibition triggered EMT and aggravated TGFβ2-induced EMT of LECs. Primary LECs were transfected with siNC or siLSS for 18 hours and further treatment with or without TGFβ2 (T2) for 48 hours. (**A**, **B**) Western blot analysis and densitometry quantification showed protein levels of LSS, ZO1, E-cad, FN, and α-SMA in the siNC, siNC+T2, siLSS, and siLSS+T2 groups. (**C**) qPCR analysis of the mRNA expression levels of FN and α-SMA in each group. qPCR analysis is presented relative to the GAPDH expression data. (**D**) Immunofluorescent staining of ZO1(*green*), FN (*red*), and α-SMA (*red*) merged with DAPI (*blue*) in each group. Representative images of three replicated experiments were presented. All scale bars, 100 µm. $^{**}P < 0.01$; $^{***}P < 0.001$. Data are shown as mean ± SD ($n = 3$).

Overexpression of LSS Prevented TGFβ2-Induced EMT of LECs and Maintained Lens Epithelial Phenotypes

Then, we explored whether the upregulation of LSS expression could prevent LECs from TGFβ2-induced EMT. As expected, overexpression of LSS in LECs inhibited the expression of mesenchymal markers, FN and α-SMA, induced by TGFβ2, and maintained expression levels of epithelial markers, ZO1 and E-cad, under TGFβ2 stimulation (Figs. 3A–C). Meanwhile, immunofluorescent staining verified that the overexpression of LSS kept LECs from mesenchymal transition and maintained epithelial morphology and cell-to-cell connections (Fig. 3D). Collectively, the overexpression of LSS prevented LECs from TGFβ2-induced EMT and sustained the lens epithelial features.

Knockdown of LSS Induced EMT by Activating Smad2/3 Signals in LECs

We continued to investigate the underlying mechanisms of LSS in regulating EMT of LECs. The canonical TGFβ2/Smad2/3 signaling has been identified to play a pivotal role in the pathogenesis of fibrotic disorders.[9,24] In this study, TGFβ2 treatment was found to induce phosphorylation of Smad2/3 and promote Smad2/3 translocation into nucleus of LECs, confirming that Smad2/3 signals were activated by TGFβ2 with potential roles in fibrotic cataracts (Supplementary Figs. S1A–C). We then examined the effect of LSS on Smad2/3 signaling activation in LECs and found that LSS inhibition significantly induced phosphorylation of Smad2/3 with increased translocation into nucleus compared to the siNC group, and knockdown of LSS

Investigative Ophthalmology & Visual Science

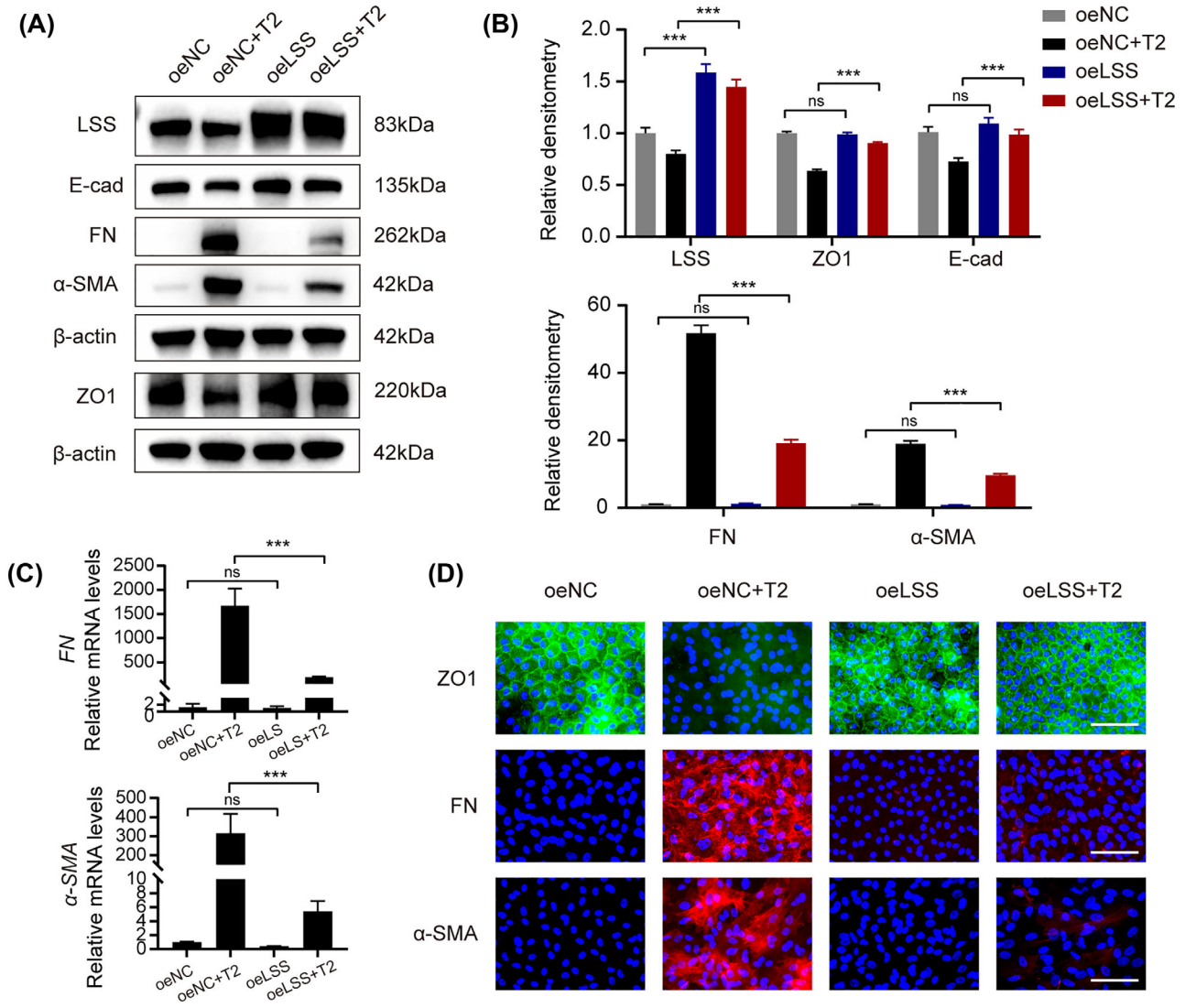

Figure 3. Overexpression of LSS suppressed TGFβ2-induced EMT and maintained LECs phenotypes. Primary LECs were transfected with oeNC or oeLSS for 18 h and further treatment with or without TGFβ2 (T2) for 48 h. (**A**, **B**) Western blot analysis and densitometry quantification showed protein levels of LSS, ZO1, E-cad, FN, and α-SMA in oeNC, oeNC+T2, oeLSS, and oeLSS+T2 groups. (**C**) qPCR analysis of the mRNA expression levels of FN and α-SMA in each group. qPCR analysis is presented relative to the GAPDH expression data. (**D**) Immunofluorescent staining of ZO1 (*green*), FN (*red*), and α-SMA (*red*) merged with DAPI (*blue*) in each group. Representative images of three replicated experiments were presented. All scale bars, 100 µm. ns, not significant. ***$P < 0.001$. Data are shown as mean ± SD ($n = 3$).

aggravated the phosphorylation of Smad2/3 and its nucleus translocation under TGFβ2-treated conditions (Figs. 4A–C). In contrast, overexpression of LSS suppressed TGFβ2-induced Smad2/3 phosphorylation and its translocation into the nucleus of LECs compared to the oeNC+T2 group (Figs. 4D–F). Together, these results revealed that knockdown of LSS induced EMT by activation of the Smad2/3 signals, and the overexpression of LSS could prevent TGFβ2-induced EMT by inhibiting phosphorylation and nucleus translocation of Smad2/3 in LECs.

SREBP1 Upregulation by LSS Exerted Suppressive Effects on TGFβ2-Induced EMT

SREBP1 is the key transcription factor in regulating sterol and fatty acid synthesis.[25] SREBP1 precursor, the full-length SREBP1 (fSREBP1), exists in an inactive state bound to the endoplasmic reticulum.[26] Upon stimulation, such as a low level of sterols, insulin, and high glucose,[27,28] fSREBP1 traffics to the Golgi and then undergoes a two-step proteolytic cleavage to release the mature SREBP1 protein (also named nuclear-localized SREBP1 [nSREBP1]), which translocates into the nucleus and activates the downstream genes expression.[25,29] According to our RNA sequencing analysis, SREBP1 was found to be downregulated in HLEEs upon TGFβ2 treatment, and sterol and lipid biosynthesis pathways were disturbed and accompanied with loss of cell–cell adhesion during lens epithelium fibrosis (Figs. 1A, B). We then investigated whether the steroid biosynthesis pathway was involved in LSS-mediated EMT of LECs. Western blot analysis identified that the protein levels of SREBP1 were decreased by TGFβ2 in a dose-dependent manner (Figs. 5A, B) or by LSS inhibition with or without TGFβ2 (Figs. 5C,

Investigative Ophthalmology & Visual Science

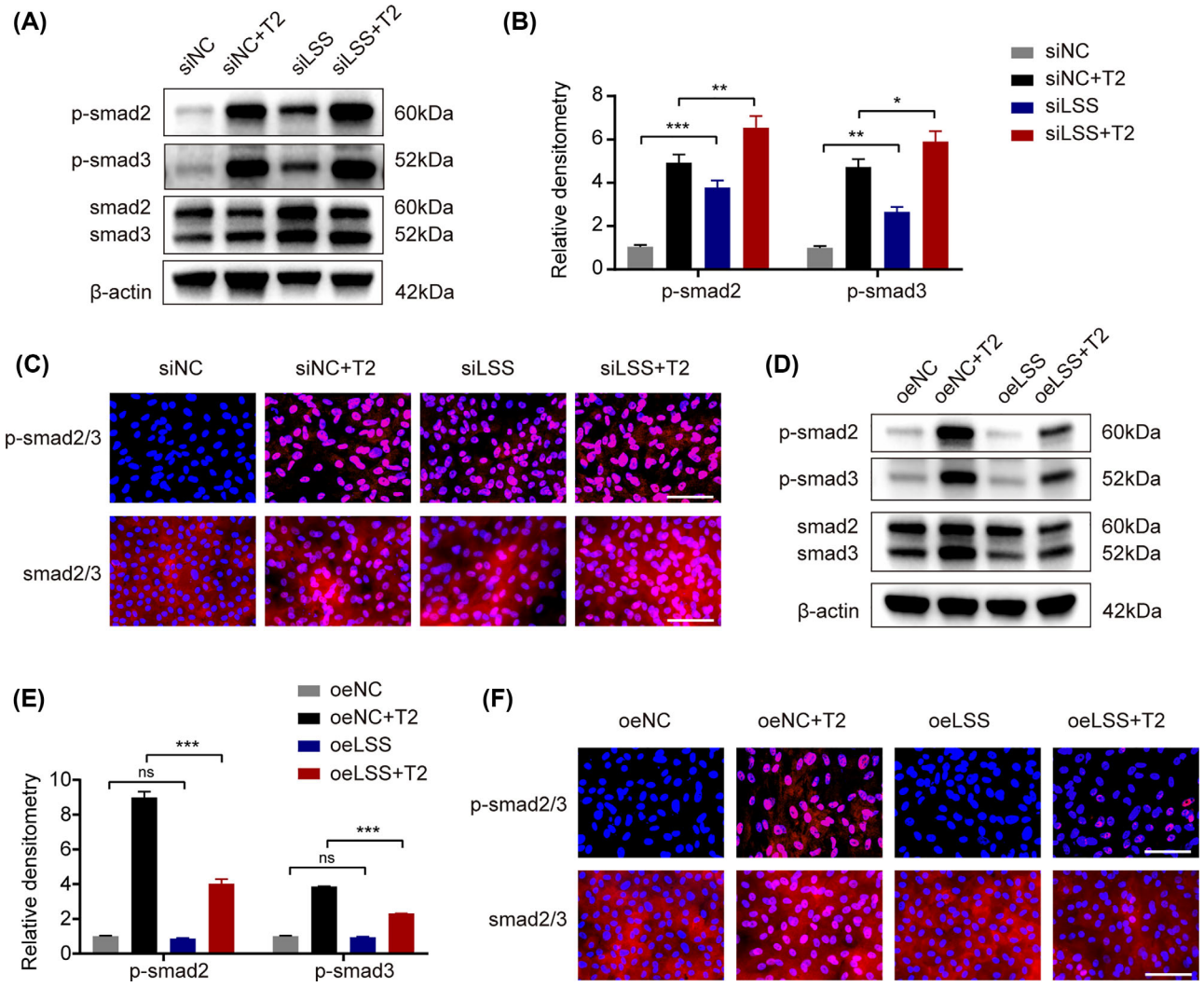

Figure 4. LSS regulated the TGFβ2/Smad2/3 signaling. Total proteins extracted from LECs were collected and p-smad2; p-smad3 as well as smad2/3 were then detected after siRNA (siNC or siLSS) transfection for 18 hours and further treatment with or without TGFβ2 for 48 hours. (**A**, **B**) Western blot analysis and densitometry quantification showed protein levels of p-smad2 (phosphorylation of smad2) and p-smad3 (phosphorylation of smad3) in the siNC, siNC+T2, siLSS, and siLSS+T2 groups. (**C**) Immunofluorescent staining of p-smad2/3 (*red*) and smad2/3 (*red*) merged with DAPI (*blue*) in siNC, siNC+T2, siLSS, and siLSS+T2 groups. (**D**, **E**) Western blot analysis and densitometry quantification showed protein levels of p-smad2 and p-smad3 (phosphorylation of Smad2/3) in oeNC, oeNC+T2, oeLSS, and oeLSS+T2 groups. (**F**) Immunofluorescent staining of p-smad2/3 (*red*) and smad2/3 (*red*) merged with DAPI (*blue*) in oeNC, oeNC+T2, oeLSS, and oeLSS+T2 groups. Representative images of three replicated experiments were presented. All scale bars, 100 µm. ns, not significant. $^{*}P < 0.05$; $^{**}P < 0.01$; $^{***}P < 0.001$. Data are shown as mean ± SD ($n = 3$).

D). By contrast, overexpression of LSS increased the protein levels of fSREBP1 and nSREBP1 (Figs. 5E, F), as well as promoted its nucleus translocation in LECs (Figs. 5G, H) with or without TGFβ2 treatment. Hence, these results imply that SREBP1 and the sterol biosynthesis pathway might be involved in EMT and LECs maintenance.

Accordingly, we then explored the effect of SREBP1 on EMT of LECs. Knockdown of SREBP1 in LECs resulted in severe decrease of epithelial markers (ZO1 and E-cad) and significant increase of mesenchymal markers (FN and α-SMA) (Figs. 6A–C; Supplementary Figs. S2A, B). Moreover, knockdown of SREBP1 promoted the Smad2/3 phosphorylation and nucleus translocation (Supplementary Figs. S3A–C) of LECs induced by TGFβ2. In contrast, SREBP1 overexpression significantly increased the expression of fSREBP1 and nSREBP1 with enhanced nucleus translocation (Figs. 6D–F), and suppressed the expression of mesenchymal markers and maintained the expression of epithelial markers (Figs. 6G, H; Supplementary Figs. S2C, D) by inhibiting Smad2/3 signals (Supplementary Figs. S3D–F).

Lanosterol Treatment Inhibited EMT of LECs by Attenuating Smad2/3 Signal Activation

Lanosterol, the catalytic product of LSS, has been proved to reverse cataract by resolving aggregated crystallins.[18] In this study, we continued to investigate the effect of lanosterol on fibrotic cataract and explore whether lanosterol could protect lens from opacity by maintaining lens epithelial homeostasis. LECs were treated with lanosterol for 72 hours with or without TGFβ2. As shown in Figure 7A, lanosterol

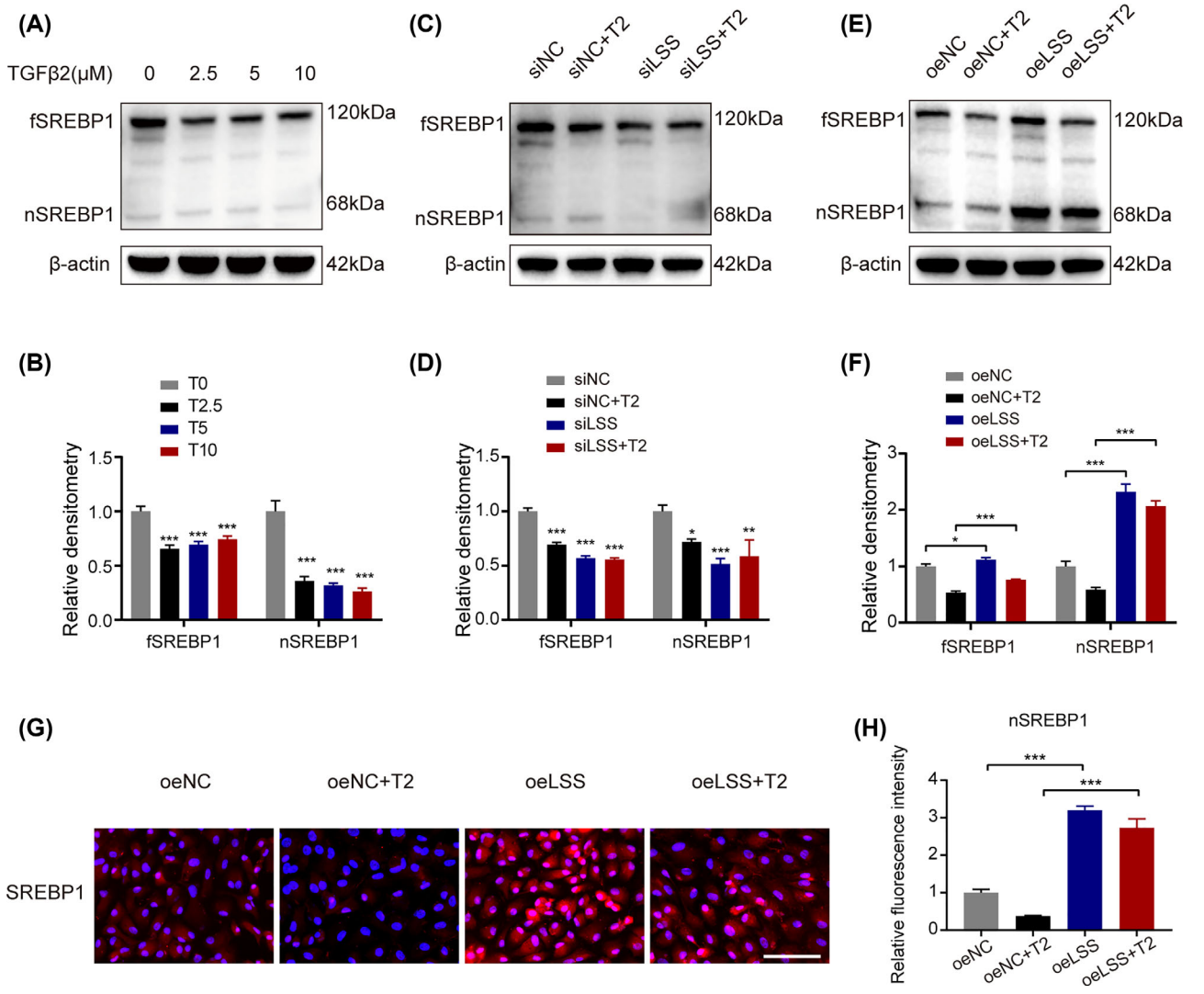

Figure 5. The expression of SREBP1 in LECs was regulated by TGFβ2 and LSS. (**A**, **B**) Western blot analysis and densitometry quantification showed protein levels of fSREBP1 and nSREBP1 in LECs treated with TGFβ2 (2.5 ng/mL, 5 ng/mL, or 10 ng/mL) for 3 days. (**C**, **D**) Western blot analysis and densitometry quantification showed protein levels of fSREBP1 and nSREBP1 in siNC, siNC+T2, siLSS, and siLSS+T2 groups. (**E**, **F**) Western blot analysis and densitometry quantification showed protein levels of fSREBP1 and nSREBP1 in the oeNC, oeNC+T2, oeLSS, and oeLSS+T2 groups. (**G**) Immunofluorescent staining of SREBP1 (*red*) merged with DAPI (*blue*) in oeNC, oeNC+T2, oeLSS, and oeLSS+T2 groups. (**H**) Relative fluorescence intensity of nSREBP1 in the oeNC, oeNC+T2, oeLSS, and oeLSS+T2 groups. Fluorescence intensity is relative to the oeNC group. Representative images of three replicated experiments were presented. All scale bars, 100 μm. $^{*}P < 0.05$; $^{**}P < 0.01$; $^{***}P < 0.001$. Data are shown as mean ± SD ($n = 3$).

maintained LECs morphology as well as cell–cell adhesion and tight junctions among LECs and prevented mesenchymal transition of LECs under TGFβ2-treated conditions. In addition, lanosterol sustained the protein expression levels of epithelial cell–cell junctions (ZO1 and E-cad) among LECs and significantly inhibited the expression of mesenchymal markers (FN and α-SMA) induced by TGFβ2 (Figs. 7B–D). Mechanically, lanosterol significantly increased the protein levels of both fSREBP1 and nSREBP1 (Supplementary Fig. S4) and prevented Smad2/3 phosphorylation as well as its translocation to nucleus in LECs with TGFβ2 administration (Figs. 7E–G).

We then moved on to investigate whether lanosterol mediated the regulatory effect of LSS on EMT. LECs were transfected with siRNA of LSS for 18 hours and then treated with lanosterol for 72 hours. The LECs morphology and LEC–cell junctions were sustained by lanosterol after knockdown of LSS (Figs. 8A–C). In addition, lanosterol reduced the expression levels of mesenchymal markers (Fig. 8B) as well as the phosphorylation and nucleus translocation of Smad2/3 (Figs. 8D–G).

Taken together, lanosterol prevented LECs from EMT induced by TGFβ2 or LSS inhibition by alleviating Smad2/3 signals activation.

Lanosterol Alleviated Rat Lens Epithelial Fibrosis and Restored Lens Transparency via Suppressing EMT of LECs

To further verify the therapeutic potential of lanosterol on lens epithelial fibrosis, we established a TGFβ2-induced

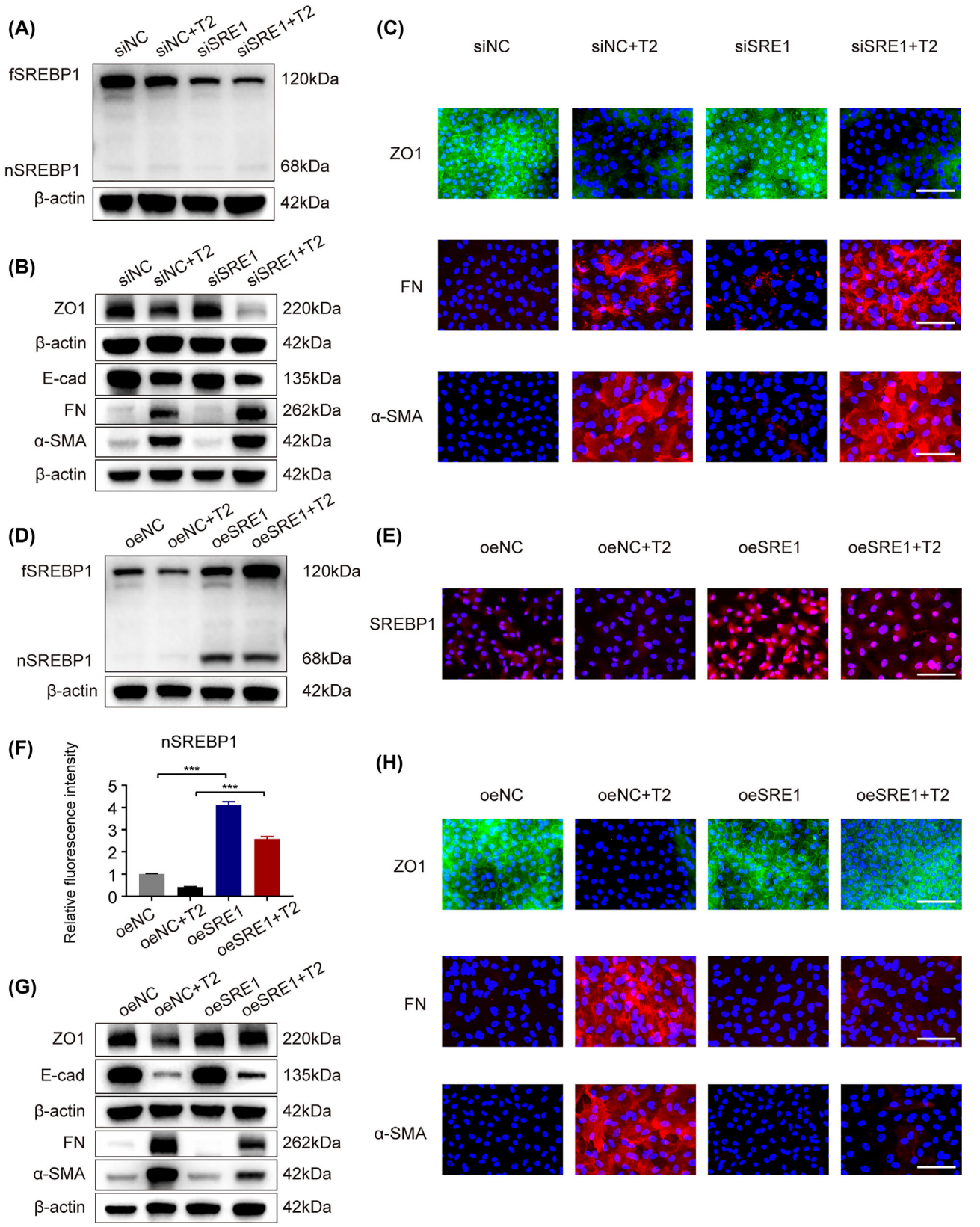

Figure 6. SREBP1 regulated EMT of LECs. Primary LECs were transfected with siNC, siSRE1, oeNC, or oeLSS for 18 hours and further treatment with or without TGFβ2 (T2) for 48 hours. (**A**) Western blot analysis showed protein levels of fSREBP1 and nSREBP1 in siNC, siNC+T2, siSRE1, and siSRE1+T2 groups. siSRE1, silencing of SREBP1; siSRE1+T2, silencing of SREBP1 and treated with TGFβ2. (**B**) Western blot analysis showed protein levels of LSS, ZO1, E-cad, FN, and α-SMA in siNC, siNC+T2, siSRE1, and siSRE1+T2 groups. (**C**) Immunofluorescent staining of ZO1 (*green*), FN (*red*), and α-SMA (*red*) merged with DAPI (*blue*) in siNC, siNC+T2, siSRE1, and siSRE1+T2 groups. (**D**) Western

Investigative Ophthalmology & Visual Science

blot analysis showed protein levels of fSREBP1 and nSREBP1 in oeNC, oeNC+T2, oeSRE1, and oeSRE1+T2 groups. oeSRE1, overexpression of SREBP1; oeSRE1+T2, overexpression of SREBP1 and treated with TGFβ2. (**E**) Immunofluorescent staining of SREBP1 (*red*) merged with DAPI (*blue*) in oeNC, oeNC+T2, oeSRE1, and oeSRE1+T2 groups. (**F**) Relative fluorescence intensity of nSREBP1 in oeNC, oeNC+T2, oeSRE1, and oeSRE1+T2 groups. Fluorescence intensity is relative to the oeNC group. (**G**) Western blot analysis showed protein levels of LSS, ZO1, E-cad, FN, and α-SMA in oeNC, oeNC+T2, oeSRE1, and oeSRE1+T2 groups. (**H**) Immunofluorescent staining of ZO1 (*green*), FN (*red*), and α-SMA (*red*) merged with DAPI (*blue*) in oeNC, oeNC+T2, oeSRE1, and oeSRE1+T2 groups. Representative images of three replicated experiments were presented. All scale bars, 100 µm. $^{***}P < 0.001$. Data are shown as mean ± SD ($n = 3$).

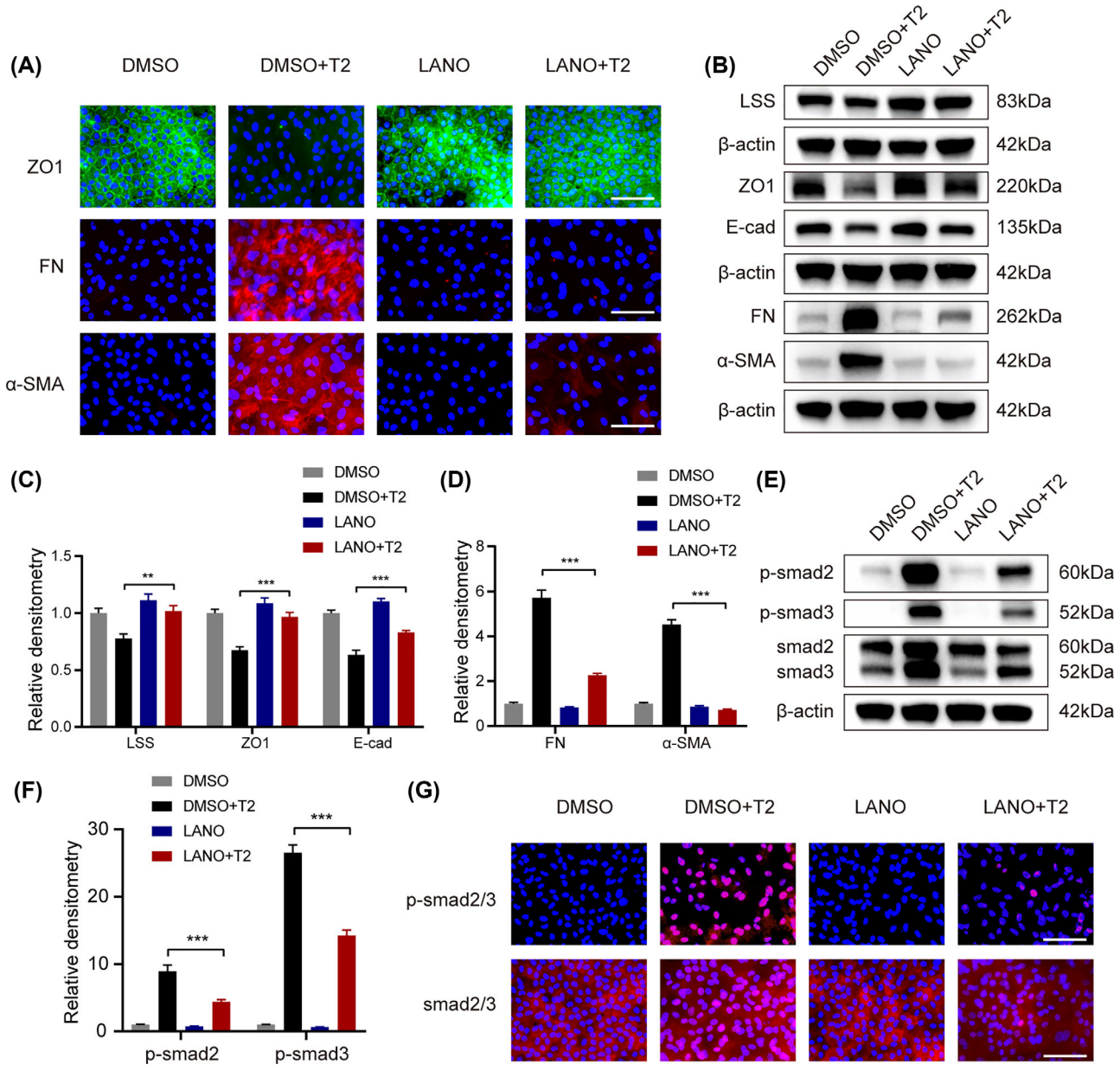

Figure 7. Lanosterol treatment prevented LECs from EMT induced by TGFβ2. Primary LECs were treated with TGFβ2 for 72 hours with DMSO or lanosterol. (**A**) Immunofluorescent staining of ZO1(*green*), FN (*red*), and α-SMA (*red*) merged with DAPI (*blue*) in DMSO, DMSO+T2, LANO, and LANO+T2 groups. LANO, lanosterol. Scale bars, 100 µm. (**B**) Western blot analysis showed protein levels of LSS, ZO1, E-cad, FN, and α-SMA in each group. (**C**, **D**) Densitometry quantification of the protein levels of LSS, ZO1, E-cad, FN, and α-SMA in each group. (**E**, **F**) Western blot analysis and densitometry quantification showed protein levels of p-smad2 and p-smad3 in each group. (**G**) Immunofluorescent staining of p-smad2/3 (*red*) and smad2/3 (*red*) merged with DAPI (*blue*) in each group. Scale bars, 100 µm. Representative images of three replicated experiments were presented. $^{**}P < 0.01$; $^{***}P < 0.001$. Data are shown as mean ± SD ($n = 3$).

fibrotic cataract model by applying the semi in vivo whole lens systems. Lenses from 3-week-old rats were treated with TGFβ2 for 6 days and obvious white plaques were observed beneath the anterior capsule (Fig. 9A). Histological analysis by hematoxylin and eosin and immunofluorescent staining of the lenses showed that the monolayered LECs transformed

Investigative Ophthalmology & Visual Science

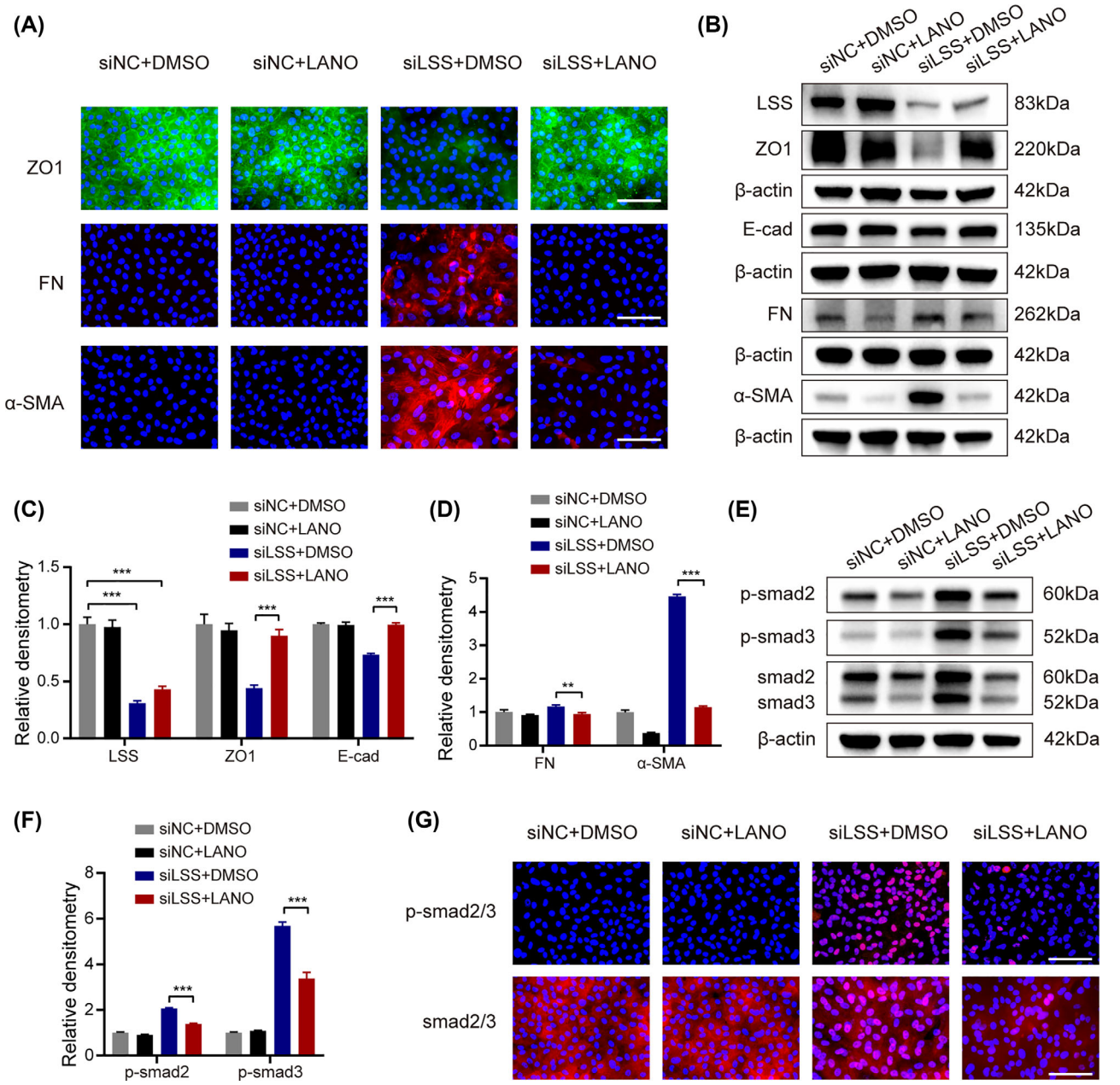

Figure 8. Lanosterol treatment prevented LECs from EMT induced by knockdown of LSS. Primary LECs were transfected with siNC or siLSS for 18 hours and further treatment with or without lanosterol for 72 hours. (**A**) Immunofluorescent staining of ZO1 (*green*), FN (*red*), and α-SMA (*red*) merged with DAPI (*blue*) in siNC+DMSO, siNC+LANO, siLSS+DMSO, and siLSS+LANO groups. Scale bars, 100 µm. (**B**) Western blot analysis showed protein levels of LSS, ZO1, E-cad, FN, and α-SMA in each group. (**C**, **D**) Densitometry quantification of the protein levels of LSS, ZO1, E-cad, FN, and α-SMA in each group. (**E**, **F**) Western blot analysis and densitometry quantification showed protein levels of p-smad2 and p-smad3 in each group. (**G**) Immunofluorescent staining of p-smad2/3 (*red*) and smad2/3 (*red*) merged with DAPI (*blue*) in each group. Scale bars, 100 µm. Representative images of three replicated experiments were presented. $^{**}P < 0.01$; $^{***}P < 0.001$. Data are shown as mean ± SD ($n = 3$).

into disorganized clumps of mesenchymal cells with excessive proliferation and invasive migration into the underlying lens fibers after TGFβ2 administration (Figs. 9B, C). The opacity clumps were further identified by a prominent accumulation of mesenchymal markers (FN and α-SMA) and abolished epithelial cell–cell junction proteins (ZO1), as well as a significant decrease of LSS protein as shown by immunofluorescent staining of both freshly cut sections of the whole lens tissues and the lens capsule whole-mounts (Figs. 9C, D) as well as verified by Western blot analysis of the LECs isolated from the whole lenses (Figs. 9E, F). Excitingly, lanosterol treatment significantly prevented LECs from TGFβ2-induced EMT and largely decreased the formation of white plaques (Fig. 9A) so as to maintain the single layer of cuboidal LECs and lens transparency, vindicating by its suppressive role in mesenchymal proteins accumulation in LECs and protective effect of lens epithelial morphology and cell–cell adhesions (Figs. 9B–F). Furthermore, we also found that lanosterol significantly inhibited Smad2/3 phosphorylation in LECs from the treated lenses during TGFβ2-induced

Investigative Ophthalmology & Visual Science

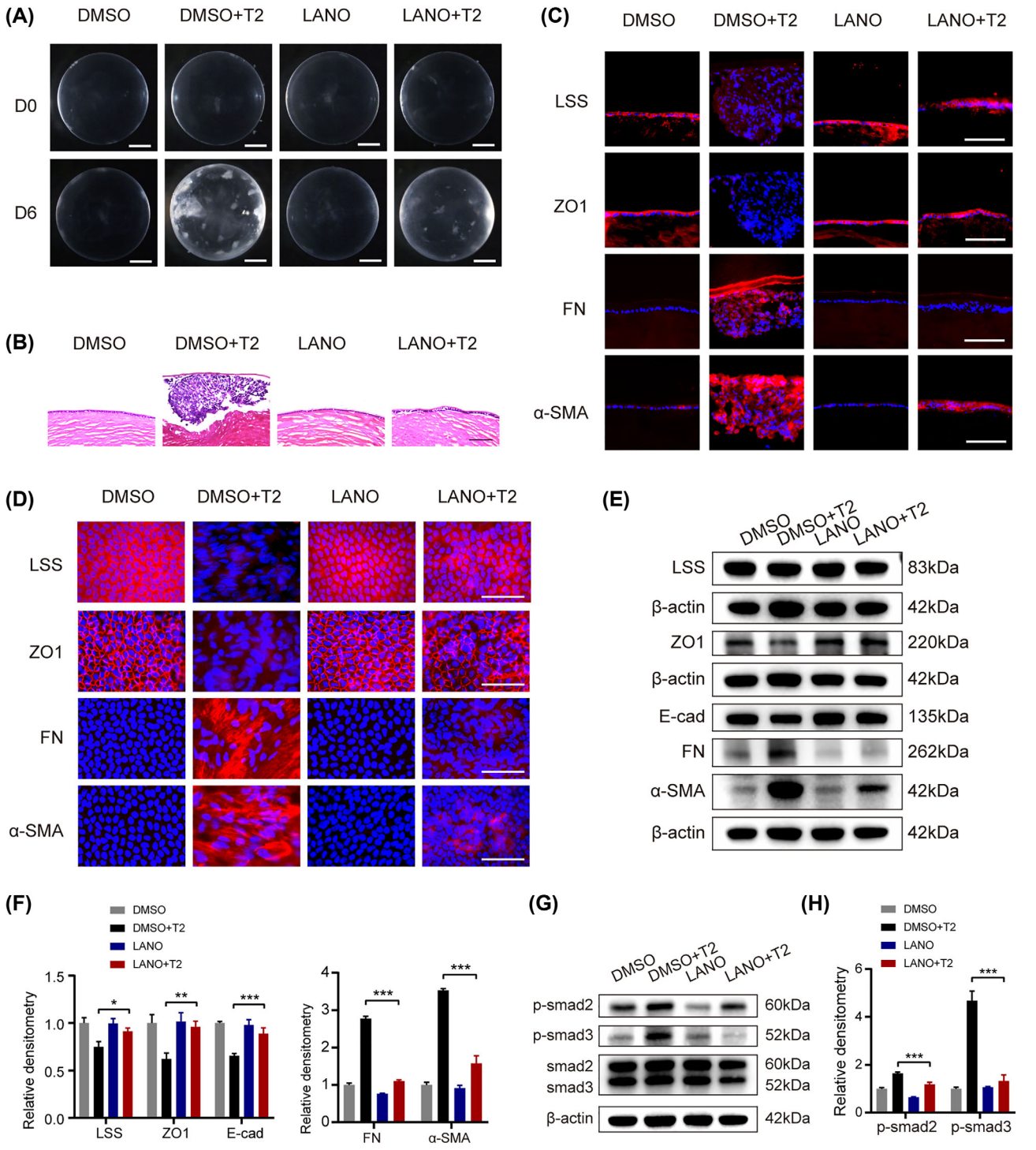

Figure 9. Lanosterol alleviated rat lens fibrosis induced by TGFβ2. Rat lenses were treated with TGFβ2 and co-treated with DMSO or lanosterol for 6 days. (**A**) Representative images of cultured rat lenses in DMSO, DMSO+T2, LANO, and LANO+T2 groups. All scale bars, 1 mm. (**B**) Hematoxylin and eosin staining of rat lenses in each group. Scale bars, 100 µm. (**C**) Immunofluorescent staining of LSS (*red*), ZO1 (*red*), FN (*red*), and α-SMA (*red*) merged with DAPI (*blue*) in rat lenses. All scale bars, 100 µm. (**D**) Immunofluorescent staining of LSS (*red*), ZO1 (*red*), FN (*red*), and α-SMA (*red*) merged with DAPI (*blue*) in rat lens anterior capsule whole mounts. All scale bars, 100 µm. (**E**, **F**) Western blot analysis and densitometry quantification showed protein levels of LSS, ZO1, E-cad, FN, and α-SMA in rat lenses of each group. (**G**, **H**) Western blot analysis and densitometry quantification showed protein levels of p-smad2 and p-smad3. Representative images of three replicated experiments were presented. $^{*}P < 0.05$; $^{**}P < 0.01$; $^{***}P < 0.001$. Data are shown as mean ± SD ($n = 3$).

Investigative Ophthalmology & Visual Science

EMT (Figs. 9G, H). Collectively, these findings revealed that lanosterol could maintain lens transparency by suppressing TGFβ2-induced EMT and fibrotic cataracts.

Discussion

Lens fibrosis could lead to opacification and vision impairment; it is, therefore, of great clinical significance to explore novel strategies for fibrotic cataracts by investigating in-depth insights into biological mechanisms behind the profibrotic EMT process. This study for the first time investigated the role of that LSS, a rate-limiting enzyme in the sterol biosynthesis, in the maintenance of lens epithelial properties by preventing of EMT via blockading the Smad2/3 signaling.

LECs, the principal cells of the lens, could proliferate and differentiate into lens fibers during lens development and maintain lens lifelong homeostasis and transparency through material transport, synthesis and metabolism.[2] LSS catalyzes the conversion of (S)-2,3-oxidosqualene to lanosterol, which is a key intermediate metabolite in sterol synthesis pathway. Cholesterol is one of the lipids that constitute plasma membrane and fulfills crucial roles in cell functions, including cell–cell adhesions, cell signaling transduction, membrane protein trafficking, and cell growth.[30,31] During lens development, the synthesis of large amounts of plasma membrane components, including cholesterol, is needed to meet the demand for the production of newly formed cell membranes during LECs differentiation into lens fibers.[32] The adult eye lens depends mostly on de novo cholesterol biosynthesis to meet the needs for cellular cholesterol, because of the extremely low cholesterol content in the aqueous humor and the limited uptake of cholesterol from plasma.[33] Mutations in enzymes of sterol biosynthesis and metabolism could cause many congenital diseases and cataracts have been reported as common complications of these diseases, such as Smith–Lemli–Opitz syndrome,[34,35] desmosterolosis,[36] and lathosterolosis.[37] Our previous study has identified that patients with *LSS* missense mutations (W581R and G588S) could develop severe total cataract with both cortical and nuclear opacity by whole exome sequencing and revealed that W581R and G588S mutations impaired the key catalytic functions of LSS and failed to prevent intracellular protein aggregation of various cataract-causing mutant crystallins.[18] Moreover, we also found that animals with *Lss* mutations exhibited cataract plaque mainly in the nucleus of lens due to altered expression and localization of Pax6 and Prox1 in lens fiber differentiation during lens development of $Lss^{G589S/G589S}$ mice.[19] The lens-specific *Lss* knockout ($Lss^{f/f-}$*Pax6*) mice showed small cloudy lenses with lens swelling and liquefaction.[38] Shumiya cataract rat with combination of *Lss* and farnesyl-diphosphate farnesyltransferase 1 (*Fdft1*)-mutant alleles developed mature cataract at approximately 11 weeks of age, showing opacity from the perinuclear zone to the cortical intermediate layer.[39] These studies have indicated multifunctional roles of LSS in lens development and maintenance by preventing protein aggregation or supporting the process of lens fiber cell differentiation during lens development. However, the roles and the underlying mechanism of LSS in EMT of LECs and fibrotic cataracts have not been explored.

Therefore, we first explored the alterations of LSS in EMT of LECs. RNA sequencing data revealed that the expression of LSS was significantly downregulated and sterols biosynthesis processes were inhibited in HLEEs upon TGFβ2 treatment. Our studies on primary LECs further validated the decrease of LSS in LECs during the EMT process. Loss- and gain-of-function studies were performed to investigate the effects of LSS on epithelial cell phenotypes of LECs, showing that knockdown of LSS in LECs could induce EMT directly, even without TGFβ2, whereas the overexpression of LSS prevented LECs from abnormal mesenchymal transition induced by TGFβ2. These results suggest that the endogenous LSS might be indispensable for maintaining the epithelial phenotypes of LECs by suppressing EMT.

The canonical TGFβ/Smad2/3 signaling pathway plays an important role in the development of fibrotic diseases.[40,41] Receptor-regulated Smads, Smad2 and Smad3, are phosphorylated in response to increased TGFβ2. The phosphorylation of Smad2 and Smad3 combine with Smad4 to form a Smad complex, which then translocates into the nucleus and regulates downstream gene transcription.[42–44] Here, we found that knockdown of LSS resulted in activation of Smad2/3 and induced expressions of mesenchymal-related proteins, which was consistent with the effect of TGFβ2 on LECs during EMT induction. By contrast, the overexpression of LSS rescued TGFβ2-induced EMT by inhibiting the activation of Smad2/3.

To clarify whether sterol biosynthesis participated in the regulation of EMT by LSS, we examined the alternations of SREBP1. SREBP1 is a key transcription factor in regulating sterol and fatty acid synthesis and has been reported to be involved in multiple fibrotic diseases and cancer metastasis.[13,45,46] Previous studies reported that SREBP1 showed different roles during the EMT process. For instance, increased SREBP1 expression was found in breast cancer and promoted cell metastasis by forming a co-repressor complex with Snail and HDAC1/2 to induce EMT.[47] Other studies showed that asiatic acid ameliorated renal fibrosis by upregulating the expression of activated SREBP1, which attenuated oxidative stress and rebalanced the disorder of the TGFβ/Smad and Wnt/β-catenin signaling pathways to repress EMT by activating peroxisome proliferator-activated receptor-γ.[48] In this study on fibrotic cataracts, we identified that both TGFβ2 treatment and knockdown of LSS could lead to the downregulation of SREBP1, whereas the overexpression of LSS significantly increased both fSREBP1 and nSREBP1 protein levels in LECs. Furthermore, we demonstrated that knockdown of SREBP1 significantly enhanced TGFβ2-induced EMT by activation of Smad2/3 signals, whereas the overexpression of SREBP1 suppressed TGFβ2-induced EMT by inhibiting the activation of Smad2/3. Further research in cross-talk of sterol biosynthesis pathway and EMT regulation would also be very interesting in the future in lens fibrosis and other fibrotic diseases.

As the direct product of LSS, lanosterol has been reported to restore lens transparency by clearance of misfolded or aggregated crystallins.[18] Here, we first discovered that lanosterol could protect LECs from EMT induced by TGFβ2 or knockdown of LSS by attenuating Smad2/3 signaling. Excitingly, lanosterol significantly decreased the formation of white fibrotic plaques and restored lens transparency by preventing LECs from EMT in the semi in vivo fibrotic cataract model. The LECs morphology as well as cell–cell adhesions and junctions were well-preserved to sustain the monolayered lens epithelium homeostasis after lanosterol treatment during TGFβ2-induced lens fibrosis. Hence, our study extended the insight into the role and mechanism of lanosterol in maintaining lens transparency by revealing a novel protective effect of lanosterol on epithelial integrity of LECs through inhibiting EMT in addition to its

Investigative Ophthalmology & Visual Science

role in alleviating cataract via re-dissolving the aggregated crystallins.

We also detected changes in the protein levels of SREBP1 in LECs after lanosterol treatment with or without TGFβ2. Consistent with the effects of LSS overexpression on SREBP1 in LECs, we found that the protein levels of both fSREBP1 and nSREBP1 were increased by lanosterol especially under the TGFβ2-treated condition (Supplementary Fig. S4). This result indicated that lanosterol might mediate the effect of LSS on increases in SREBP1 levels to initiate sterol biosynthesis so as to protect cellular homeostasis upon sensing the stimulation signals such as TGFβ2. Furthermore, in addition to lanosterol, other downstream sterol products of LSS and related mechanisms might also be involved in regulating the EMT of LECs, which deserve further exploration in the future.

Taken together, we identified a novel role and mechanism of LSS in sustaining lens epithelium homeostasis and lens transparency by preventing LECs from EMT (Supplementary Fig. S5). LSS expression and sterol biosynthesis processes were first found to be decreased during lens epithelial fibrosis. LSS inhibition could directly induce EMT by activation of Smad2/3 signals, while overexpression of LSS rescued TGFβ2-induced EMT and maintain the LECs phenotypes. In addition, LSS could alter the expression of SREBP1, a key transcription factor for sterol biosynthesis, and its upregulation effectively protected LECs from EMT via suppressing Smad2/3 activation. Furthermore, we first identified that lanosterol, the catalytic product of LSS and a key precursor of sterol biosynthesis, exhibited therapeutic effects on lens fibrosis by suppressing EMT of LECs. Our study demonstrated for the first time that LSS and related-sterol synthesis pathways played important roles in preventing lens fibrosis via maintaining lens epithelium integrity by protecting LECs from EMT, providing potential novel therapeutic strategies for fibrotic cataracts and other fibrotic diseases.

Acknowledgments

Supported by National Natural Science Foundation of China (No. 82070944, No. 81721003), the State Key Laboratory of Ophthalmology, Zhongshan Ophthalmic Center, Sun Yat-Sen University.

Disclosure: **P. Ma,** None; **J. Huang,** None; **B. Chen,** None; **M. Huang,** None; **L. Xiong,** None; **J. Chen,** None; **S. Huang,** None; **Y. Liu,** None

References

1. Cicinelli MV, Buchan JC, Nicholson M, Varadaraj V, Khanna RC, Cataracts. *Lancet*. 2022;401:377–389.
2. Liu Z, Huang S, Zheng Y, et al. The lens epithelium as a major determinant in the development, maintenance, and regeneration of the crystalline lens. *Prog Retin Eye Res*. 2022;19:101112.
3. Shu DY, Lovicu FJ. Myofibroblast transdifferentiation: the dark force in ocular wound healing and fibrosis. *Prog Retin Eye Res*. 2017;60:44–65.
4. Lovicu FJ, Shin EH, McAvoy JW. Fibrosis in the lens. Sprouty regulation of TGFbeta-signaling prevents lens EMT leading to cataract. *Exp Eye Res*. 2016;142:92–101.
5. Saika S. TGFbeta pathobiology in the eye. *Lab Invest*. 2006;86:106–115.
6. Dawes LJ, Angell H, Sleeman M, Reddan JR, Wormstone IM. TGFbeta isoform dependent Smad2/3 kinetics in human lens epithelial cells: a Cellomics analysis. *Exp Eye Res*. 2007;84:1009–1012.
7. Li J, Tang X, Chen X. Comparative effects of TGF-beta2/Smad2 and TGF-beta2/Smad3 signaling pathways on proliferation, migration, and extracellular matrix production in a human lens cell line. *Exp Eye Res*. 2011;92:173–179.
8. Saika S, Okada Y, Miyamoto T, Ohnishi Y, Ooshima A, McAvoy JW. Smad translocation and growth suppression in lens epithelial cells by endogenous TGFbeta2 during wound repair. *Exp Eye Res*. 2001;72:679–686.
9. Saika S, Miyamoto T, Ishida I, et al. TGFbeta-Smad signalling in postoperative human lens epithelial cells. *Br J Ophthalmol*. 2002;86:1428–1433.
10. Saika S, Kono-Saika S, Ohnishi Y, et al. Smad3 signaling is required for epithelial-mesenchymal transition of lens epithelium after injury. *Am J Pathol*. 2004;164:651–663.
11. de Iongh RU, Wederell E, Lovicu FJ, McAvoy JW. Transforming growth factor-beta-induced epithelial-mesenchymal transition in the lens: a model for cataract formation. *Cells Tissues Organs*. 2005;179:43–55.
12. Kaminsky-Kolesnikov Y, Rauchbach E, Abu-Halaka D, et al. Cholesterol induces Nrf-2- and HIF-1alpha-dependent hepatocyte proliferation and liver regeneration to ameliorate bile acid toxicity in mouse models of NASH and fibrosis. *Oxid Med Cell Longev*. 2020;2020:5393761.
13. Dorotea D, Koya D, Ha H. Recent insights into SREBP as a direct mediator of kidney fibrosis via lipid-independent pathways. *Front Pharmacol*. 2020;11:265.
14. Zhou F, Sun X. Cholesterol metabolism: a double-edged sword in hepatocellular carcinoma. *Front Cell Dev Biol*. 2021;9:762828.
15. Gobel A, Rauner M, Hofbauer LC, Rachner TD. Cholesterol and beyond - the role of the mevalonate pathway in cancer biology. *Biochim Biophys Acta Rev Cancer*. 2020;1873:188351.
16. Borchman D, Yappert MC. Lipids and the ocular lens. *J Lipid Res*. 2010;51:2473–2488.
17. Shin S, Zhou H, He C, et al. Qki activates Srebp2-mediated cholesterol biosynthesis for maintenance of eye lens transparency. *Nat Commun*. 2021;12:3005.
18. Zhao L, Chen XJ, Zhu J, et al. Lanosterol reverses protein aggregation in cataracts. *Nature*. 2015;523:607–611.
19. Zhao M, Mei T, Shang B, et al. Defect of LSS disrupts lens development in cataractogenesis. *Front Cell Dev Biol*. 2021;9:788422.
20. Xiong L, Sun Y, Huang J, et al. Long non-coding RNA H19 prevents lens fibrosis through maintaining lens epithelial cell phenotypes. *Cells*. 2022;12:99.
21. Zhou Y, Zhou B, Pache L, et al. Metascape provides a biologist-oriented resource for the analysis of systems-level datasets. *Nat Commun*. 2019;10:1523.
22. Hales AM, Chamberlain CG, McAvoy JW. Susceptibility to TGFbeta2-induced cataract increases with aging in the rat. *Invest Ophthalmol Vis Sci*. 2000;41:3544–3551.
23. Wang X, Wang B, Zhao N, et al. Pharmacological targeting of BET bromodomains inhibits lens fibrosis via down-regulation of MYC expression. *Invest Ophthalmol Vis Sci*. 2019;60:4748–4758.
24. Lonn P, Moren A, Raja E, Dahl M, Moustakas A. Regulating the stability of TGFbeta receptors and Smads. *Cell Res*. 2009;19:21–35.
25. Shimano H, Sato R. SREBP-regulated lipid metabolism: convergent physiology - divergent pathophysiology. *Nat Rev Endocrinol*. 2017;13:710–730.
26. Goldstein JL, DeBose-Boyd RA, Brown MS. Protein sensors for membrane sterols. *Cell*. 2006;124:35–46.
27. Nakakuki M, Kawano H, Notsu T, Imada K, Mizuguchi K, Shimano H. A novel processing system of sterol regula-

Investigative Ophthalmology & Visual Science

tory element-binding protein-1c regulated by polyunsaturated fatty acid. *J Biochem*. 2014;155:301–313.
28. Cheng C, Ru P, Geng F, et al. Glucose-mediated N-glycosylation of SCAP is essential for SREBP-1 activation and tumor growth. *Cancer Cell*. 2015;28:569–581.
29. Brown MS, Goldstein JL. The SREBP pathway: regulation of cholesterol metabolism by proteolysis of a membrane-bound transcription factor. *Cell*. 1997;89:331–340.
30. Simons K, Toomre D. Lipid rafts and signal transduction. *Nat Rev Mol Cell Biol*. 2000;1:31–39.
31. Widomska J, Subczynski WK. Why is very high cholesterol content beneficial for the eye lens but negative for other organs? *Nutrients*. 2019;11(5):1083.
32. Cenedella RJ. Sterol synthesis by the ocular lens of the rat during postnatal development. *J Lipid Res*. 1982;23:619–626.
33. Cenedella RJ. Cholesterol and cataracts. *Surv Ophthalmol*. 1996;40:320–337.
34. Cotlier E, Rice P. Cataracts in the Smith-Lemli-Opitz syndrome. *Am J Ophthalmol*. 1971;72:955–959.
35. Goodwin H, Brooks BP, Porter FD. Acute postnatal cataract formation in Smith-Lemli-Opitz syndrome. *Am J Med Genet A*. 2008;146A:208–211.
36. Clayton P, Mills K, Keeling J, FitzPatrick D. Desmosterolosis: a new inborn error of cholesterol biosynthesis. *Lancet*. 1996;348:404.
37. Krakowiak PA, Wassif CA, Kratz L, et al. Lathosterolosis: an inborn error of human and murine cholesterol synthesis due to lathosterol 5-desaturase deficiency. *Hum Mol Genet*. 2003;12:1631–1641.
38. Wada Y, Kikuchi A, Kaga A, et al. Metabolic and pathologic profiles of human LSS deficiency recapitulated in mice. *PLoS Genet*. 2020;16:e1008628.
39. Mori M, Li G, Abe I, et al. Lanosterol synthase mutations cause cholesterol deficiency-associated cataracts in the Shumiya cataract rat. *J Clin Invest*. 2006;116:395–404.
40. Hu HH, Chen DQ, Wang YN, et al. New insights into TGF-beta/Smad signaling in tissue fibrosis. *Chem Biol Interact*. 2018;292:76–83.
41. Meng XM, Nikolic-Paterson DJ, Lan HY. TGF-beta: the master regulator of fibrosis. *Nat Rev Nephrol*. 2016;12:325–338.
42. Heldin CH, Miyazono K, ten Dijke P. TGF-beta signalling from cell membrane to nucleus through SMAD proteins. *Nature*. 1997;390:465–471.
43. Wrana JL. Regulation of Smad activity. *Cell*. 2000;100:189–192.
44. Lamouille S, Xu J, Derynck R. Molecular mechanisms of epithelial-mesenchymal transition. *Nat Rev Mol Cell Biol*. 2014;15:178–196.
45. Gabitova-Cornell L, Surumbayeva A, Peri S, et al. Cholesterol pathway inhibition induces TGF-beta signaling to promote basal differentiation in pancreatic cancer. *Cancer Cell*. 2020;38:567–583.e511.
46. Ayyappan JP, Lizardo K, Wang S, Yurkow E, Nagajyothi JF. Inhibition of SREBP improves cardiac lipidopathy, improves endoplasmic reticulum stress, and modulates chronic chagas cardiomyopathy. *J Am Heart Assoc*. 2020;9:e014255.
47. Zhang N, Zhang H, Liu Y, et al. SREBP1, targeted by miR-18a-5p, modulates epithelial-mesenchymal transition in breast cancer via forming a co-repressor complex with Snail and HDAC1/2. *Cell Death Differ*. 2019;26:843–859.
48. Zhang ZH, He JQ, Zhao YY, Chen HC, Tan NH. Asiatic acid prevents renal fibrosis in UUO rats via promoting the production of 15d-PGJ2, an endogenous ligand of PPAR-gamma. *Acta Pharmacol Sin*. 2020;41:373–382.